Bulletin of Geophysics and Oceanography Vol. 66, n. 1, pp. 95-112; March 2025
DOI 10.4430/bgo00461

Reservoir characterisation of Meyal-8, Meyal-9, and Meyal-10 by well log data, southern Potwar, upper Indus Basin, Pakistan

A. Kamal[1], F. Rehman[1], M. Kashif[1], B. Dou[2], M.F. Ullah[1], Y. Semab[1] and S. Khan[1]

[1] *Department of Earth Sciences, University of Sargodha, Sargodha, Pakistan*
[2] *Faculty of Engineering, China University of Geosciences, Wuhan, China*

(Received: 14 April 2023; accepted: 2 May 2024; published online: 3 March 2025)

ABSTRACT The Meyal oil field is a significant oil field in the Potwar Basin, Punjab, Pakistan. This study deals with the petrophysical analysis of the Meyal-08, Meyal-09, and Meyal-10 wells to identify suitable reservoir zones with the help of well log data. Rock physics modelling allowed quantitative prediction of the relationship between porosity, saturation, shale volume, and elastic properties. The Chorgali Formation (Eocene) is the main reservoir of the Meyal oil field. Three suitable zones of interest have been marked: zone-1 of Meyal-08 with a shale volume of 3.1%, average porosity of 32.09%, effective porosity of 31.11%, water saturation of 79.21%, average hydrocarbon saturation of 20.79%, and net pay of 53.1%; zone-1 of Meyal-09 with a shale volume of 53.79%, average porosity of 20.55%, effective porosity of 7.20%, water saturation of 44.44%, average hydrocarbon saturation of 55.56%, and net pay of 9.4%; and zone-1 of Meyal-10 with a shale volume of 21.8%, average porosity of 19.1%, effective porosity of 14.68%, water saturation of 43%, hydrocarbon saturation of 57%, and net pay of 5%. Based on all these characteristics the Meyal field results to be a very significant field for the economical production of hydrocarbon in the Potwar area.

Key words: Indus basin, Meyal oilfield, Potwar Basin, reservoir characteristics, well logging.

1. Introduction

The Potwar Basin is a significant petroliferous basin in Pakistan. Reservoir characteristics are generally related to porosity, rock composition, and the concentration of reservoir fluids (hydrocarbon) in pore volume (Dolson, 2016; Chongwain *et al.,* 2018; Bagheri and Rezaei, 2019; Singh, 2019; Sajid *et al*., 2020; Shi *et al*., 2023; Zhao *et al*., 2024). The current study mainly emphasised the prediction of the reservoir characteristics in the Potwar Basin by well log data. The Meyal field, the main hydrocarbon-producing oil field, is geographically situated in the Potwar Plateau, in the northern Punjab province of Pakistan. In 1968, Pakistan Oilfield Limited performed seismic data acquisition in the study area and discovered 16 exploratory wells. From three reservoirs in the Meyal field, 36 million barrels of oil and 250 billion cubic feet of gas have been produced. The central part of the Eocene reservoir has mainly been involved in drilling. At a depth from 11,984 to 14,084 feet, oil and gas have been produced from the Eocene Chorgali Formation, Sakesar Limestone, and Lockhart Limestone (Paleocene), Ranikot and Datta Formations (Jurrasic) (Ali *et al*., 2022).

The southern Indus basin is characterised by complex tectonic history and comprises

numerous oil and gas traps (Faisal *et al*., 2013; Rehman *et al*., 2014; Ahmed *et al.,* 2023; Ullah *et al*., 2023). It is difficult to predict the reservoir characteristics due to the high contents of salt and gypsum that create complexities, which have brought challenges for hydrocarbon exploration activities in the study area. Evaporites act as seal rock for traps. Stratigraphy, sedimentary facies and paleontology are significant tools for the prediction of the depositional environment. Reservoir characterisation is used to determine permeability, porosity, net-to-gross pay, water saturation, pore fluid, and other reservoir characteristics (Bahar and Kelkar, 2000; Hill, 2017; Cheng *et al*., 2022; Moosavi *et al*., 2022, 2023). The ascertained reservoirs consist of Eocene and Paleocene carbonate successions and Cambrian, Permian, and Jurassic clastic sediments in different fields (Akhter *et al*., 2018). The main oil generating reservoirs in the Meyal oil field are the Datta and Chorgali formations. The main objective of the study area is to: 1) demark the reservoir zone from the well log data; 2) identify and correlate the sub-surface stratigraphic sequence of the Meyal-08, Meyal-09, and Meyal-10 wells; and 3) calculate the pay zones.

2. Geological setting

The study area is situated in the Potwar area, in the upper Indus Basin in Pakistan. Tectonically the northern boundary of the Potwar Basin is marked by the Kala Chitta Range and Margalla Hills (Aamir and Siddiqui, 2006; Abir *et al.,* 2015; Amjad *et al*., 2023). To the east, it is bounded by the Jhelum River and to the west by the Indus River. The northern and southern boundaries of the basin are restricted by the Main Boundary Thrust and the Salt Range Thrust, respectively (Amjad *et al*., 2023). The studied zone is a part of the Himalayan Fold and Thrust Belt and consists of numerous anticlines and synclines (Farah and Lillie, 1989). The North Potwar Deformed Zone comprises a highly deformed and imbricated thrust sheet, and lies to the north of the Soan syncline (Dominik *et al*., 2013; Iqbal *et al.,* 2015; Awais *et al*., 2020; Yasin *et al*., 2021; Durrani *et al*., 2022).

Lithostratigraphic units, well preserved in the Potwar basin, range from Precambrian to Quaternary age sediments. These rock units were deposited from marine to fluvial depositional environments. Cretaceous and Oligocene rocks are absent while thick fluvial sediments of Murree, Kamlial Chinji, Nagri, and Dhok Pathan formations have deposited in Potwar foredeep during the main orogenic phase in Miocene and Pliocene (Fig. 1), in response to continued uplifts in the north (Sameeni *et al*., 2013; Awais *et al*., 2015; Shah and Abdullah, 2016; Khan *et al*., 2017; Mehmood *et al*., 2018; Awais *et al*., 2019; Awais *et al*., 2020).

In the study area, the Hangu Formation (Paleocene) consists of fine to coarse-grained sandstone, white to light grey and reddish brown. It also consists of carbonaceous shale and lateritic bands. The Lokhart Limestone (Paleocene), instead, consists of grey to medium grey thick bedded-massive limestone. The Patala Formation (Paleocene) consists of greenish-grey, selenite-bearing shale with subordinate limestone and coal seam. The Nammal Formation (Eocene) comprises grey shale, marl, and limestone, whereas Sakesar Limestone comprises cream to light grey nodular (chert) limestone, and the Chorgali Formation (Eocene) comprises shale and limestone. The Murree Formation consists of massive red to purple clay and greenish-grey sandstone. The Kamlial Formation (Miocene) comprises sandstone with subordinate shale, whereas the Chinji and Nagri formations (Pliocene) consist of red clays, and sandstone with subordinate conglomerates.

In the study area, shales of the Jurassic (Datta and Shinawari formations) and Paleocene

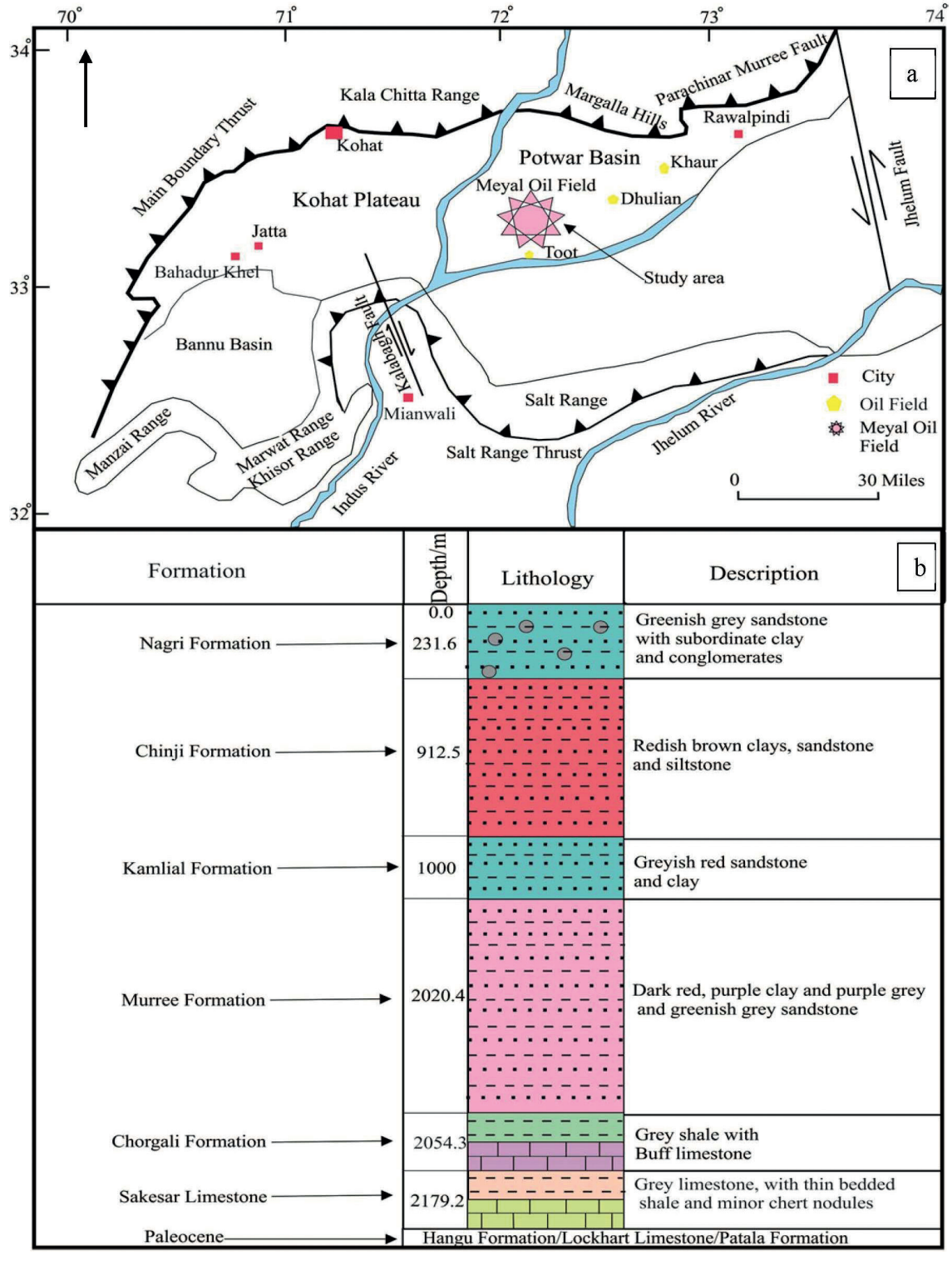

Fig. 1 - a) The geological and structural map of the Potwar Plateau (after Khan *et al.*, 1986); b) the generalised stratigraphic column of the study area.

(Patala Formation) ages act as source rock. The total organic carbon content (TOC) values range from 0.6 to 3.5%, which are mainly comprised of type II and type III kerogens (Hasany and Saleem, 2012). The Datta Sandstone, Sakesar Limestone, and Chorgali Formation act as good reservoirs, while shales of the Nammal and Kuldana formations act as cap rocks (Hasany and Saleem, 2012).

3. Methodology

Petrophysical analysis has been used to evaluate the reservoir characteristics. In GeoGraphix software, well log data, imported wherever a potential reservoir zone is identified, and separate from a non-reservoir zone, are generally based on low and profound resistivity logs, density-neutron crossovers, the presence of mud cakes, and low gamma ray (*GR*) values. The data required include the open-hole wireline-logs of Meyal-08, Meyal-09, and Meyal-10. The Log ASCII Standard files included sonic logs, density logs, GR logs, and resistivity logs.

At first, the shale baseline shows the impermeable portion of shale. On the left side, the baseline marks the clean zone of sand and limestone. In the following step, the resistivity of the fluid is determined, and shows a high resistivity in the zone of interest, proving the presence of hydrocarbon. The next step is to mark the good porous zone against the high resistivity zone. Saline water is present in rock and produced electrical conductivity. Low resistivity is caused when the water saturation increases and the hydrocarbon saturation decreases.

Shale volume can be determined with GR_{log} by applying the Schlumberger equation. Volumetrically, shale-bound water can be calculated (Asquith *et al*., 2004):

$$V_{shl} = \left(GR_{log} - GR_{min}\right)/(GR_{max} - GR_{min}) \tag{1}$$

where V_{shl} represents the shale volume, GR_{log} represents the *GR* value at a given point in the zone of interest, and GR_{min} (for clean carbonate and sand) and GR_{max} (for shale) represent, respectively, the minimum and maximum value of GR_{log} in the zone of interest.

Some common minerals, densities, and pore fluids have been calculated with (Asquith *et al*., 2004):

$$\phi_d = (\rho_{ma} - \rho_b)/\left(\rho_{ma} - \rho_f\right) \tag{2}$$

where ϕ_d is the porosity, ρ_{ma} is the density of matrix, ρ_b is the density log response, and ρ_f is the fluid density.

In the case of non-availability of a neutron log, the average porosity (ϕ_a) can also be determined by using sonic logs.

$$\begin{aligned} \phi_a &= (\phi_d - \phi_n)/2 \\ \phi_a &= (\phi_d - \phi_s)/2 \end{aligned} \tag{3}$$

where ϕ_n and ϕ_s are neutron porosity and sonic porosity, respectively.

Effective porosity ϕ_e, which includes the only pore space in the sand, may be calculated by means of (Asquith *et al*., 2004):

$$\phi_e = \phi_a \times (1 - V_{shl}). \quad (4)$$

Low shale volume values correspond to high effective porosity and vice versa.

In the zone of interest, porosity (ϕ) can be computed from sonic, neutron, and density logs. Porosity is measured in percentage between 0 and 1 and expressed as a percentage between 0 and 100%. Porosity can be calculated by means of Eqs. (3) and (4). Average porosity is a blend of density and density porosity. Density porosity of an interested zone can be calculated with the Schlumberger *et al.* (1934) equation:

$$\phi_d = (\rho_m - \rho_b)/(\rho_m - \rho_f). \quad (5)$$

Eq. (5) represents the total porosity (ϕ_d), including pore space in shale and sand with matrix density (ρ_m), being 2.65 g/cm³ for sandstone, fluid density (ρ_f), being 1.1 g/cm³ for saline water, and bulk density (ρ_b).

Total porosity is the percentage of total pore space in a rock body in relation to its bulk volume (Asquith *et al*., 2004).

The transit travel time and intergranular porosity in the formation are calculated through sonic porosity (ϕ_s):

$$\phi_S = (\Delta t - \Delta t_{ma})/(\Delta t_f - \Delta t_{ma}) \quad (6)$$

where Δt is the transit time, Δt_{ma} is the matrix sonic value, and Δt_f is the fluid sonic value.

To determine the water resistivity (*Rw*), the self potential (SP) technique has been applied.

The water saturation (S_w) has been calculated with Archie equation (Asquith *et al*., 2004):

$$S_w = \sqrt{(a/\phi^m) \times (R_w/R_t)} \quad (7)$$

where S_w is the total water saturation, i.e. the friction pore space occupied by water, R_w is the water resistivity, ϕ is the porosity, which includes the pore spaces in shale and sand, a is a constant, often taken to be 1, and m is the cementation factor.

The petrophysical analysis of all wells studied is shown in Table 1.

Eq. (7) represents the fluid constant, and R_t represents the true resistivity. Water resistivity is commonly determined in *GR* logs at its minimum value: the higher the porosity, the lower the resistivity.

Water resistivity is obtained by (Asquith *et al*., 2004):

$$R_w = (\phi_E^2 \times R_t). \quad (8)$$

where ϕ_E^2 represents the effective porosity in the clean zone and R_t, the resistivity of formation has been evaluated by the deep laterolog (LLD) curve in the clean zone.

Hydrocarbon saturation (Sh_A) can be calculated by (Asquith *et al*., 2004):

Table 1- Values used for the petrophysical analysis in the Meyal-08, Meyal-09, and Meyal-10 wells in GeoGraphix software. *DT* = true density; ϕ_e = effective porosity; *Sw* = water saturation; *a* = constant, often taken to be 1; *m* = cementation factor; *n* = saturation exponent.

Well name	GR_{max}	GR_{min}	ρ_m	ρ_f	DT_m	DT_f	*Rw*	*Rsh*	*a*	*m*	*n*	Cut-off		
												V_{shl}	ϕ_e	*Sw*
Meyal 08	140	20	2.65	1.00	55	189	0.030	0.9	11	22	2	<30%	>5%	<40%
Meyal 09	140	20	2.65	1.00	55	189	0.030	0.9	11	22	2	<30%	>5%	<40%
Meyal 10	140	20	2.65	1.00	55	189	0.030	0.9	11	22	2	<30%	>5%	<40%

$$Sh_A = 1 - S_w \quad (9)$$

where S_w represents water saturation.

Net pay thickness can be estimated by applying three cut-offs to the reservoir zone. Cut-off has been used where porosity >5%, V_{shl} <30 %, and S_w <40% (Table 1).

4. Results and discussion

4.1. Interpretation

4.1.1. Interpretation of zone-1 of the Meyal-08 well

Zone-1 of the Meyal-08 well is marked from 3,716 m to 3,730 m (14 m) (Fig. 2). Average shale volume is 3.1% (y-axis) plotted against depth/m (x-axis) (Fig. 3a), effective porosity 31.11% (y-axis) against depth/m (x-axis) (Fig. 3b), average porosity 32.09% (y-axis) plotted against depth/m (x-axis) (Fig. 3c), average water saturation (Sw_A) 79.21% (y-axis) against depth/m (x-axis) (Fig. 4a), and average hydrocarbon saturation (Sh_A) 20.79%. (y-axis) against depth/m (x-axis) (Fig. 4b). By applying three cut-offs, V_{shl}, ϕ_e, and *Sw*, it is possible to calculate the average net pay cut-off (*NETPAY*) that is 12% in the 14-metre thickness of zone-1 of the Meyal-08 well (Fig. 4c).

4.1.2. Interpretation of zone-1 of the Meyal-09 well

Zone-1 of the Meyal-09 well is marked from 3,672 to 3,687 m of depth (13 m thick) (Fig. 5). The zone of interest is demarcated in red shale of the Chorgali Formation. The calculated average shale volume is 53.79% (y-axis) plotted against depth/m (x-axis) (Fig. 6a), ϕ_e is 7.20% (y-axis) plotted against depth/m (x-axis) (Fig. 6b), ϕ_a is 20.55% (y-axis) plotted against depth/m (x-axis) (Fig. 6c), Sw_A is 44.44% (y-axis) plotted against depth/m (x-axis) (Fig. 7a), and Sh_A is 55.56% (y-axis) plotted against depth/m (x-axis) (Fig. 7b). The *NETPAY*, instead, is 9.4% (y-axis) plotted against depth/m (x-axis) (Fig. 7c), calculated from three cut-offs, V_{shl}, ϕ_e, and *Sw*, of zone-1 of the Meyal-09 well (Fig. 5).

4.1.3. Interpretation of zone-1 of the Meyal-10 well

Zone-1 of the Meyal-10 well is marked from 3,250 m to 3,265 m of depth (15-m thick) (Fig. 8). The zone of interest is demarcated in the Chorgali Formation. The calculated average

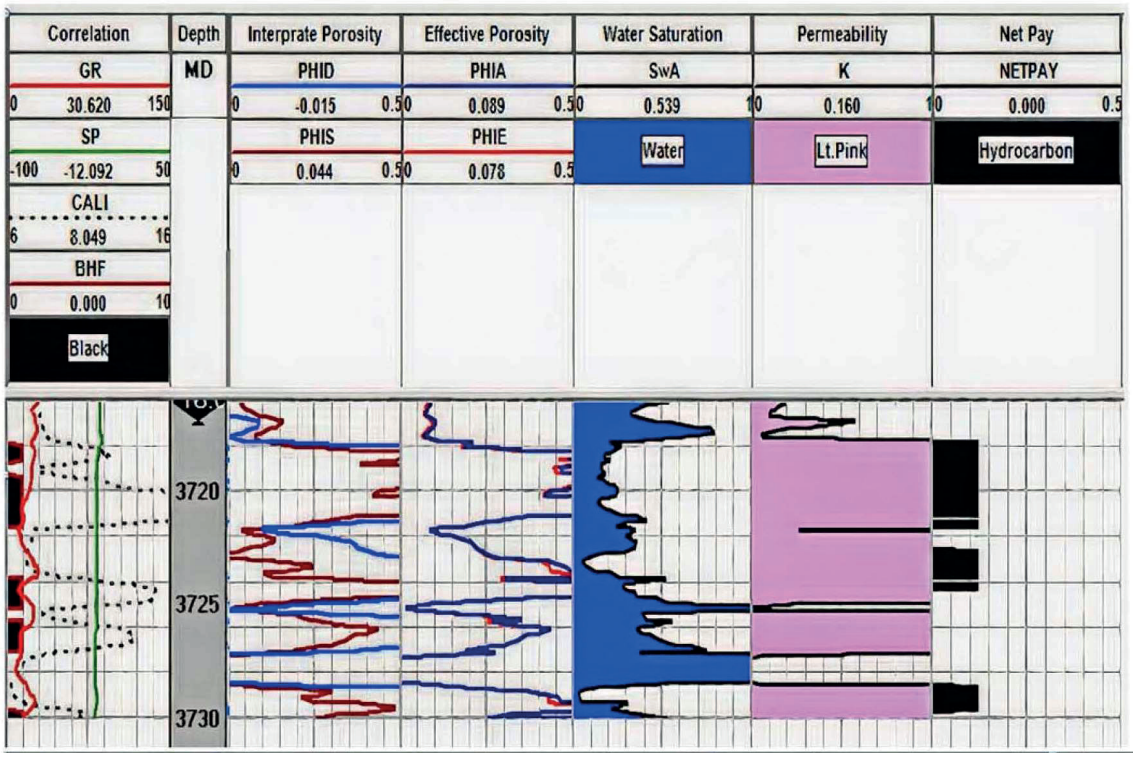

a

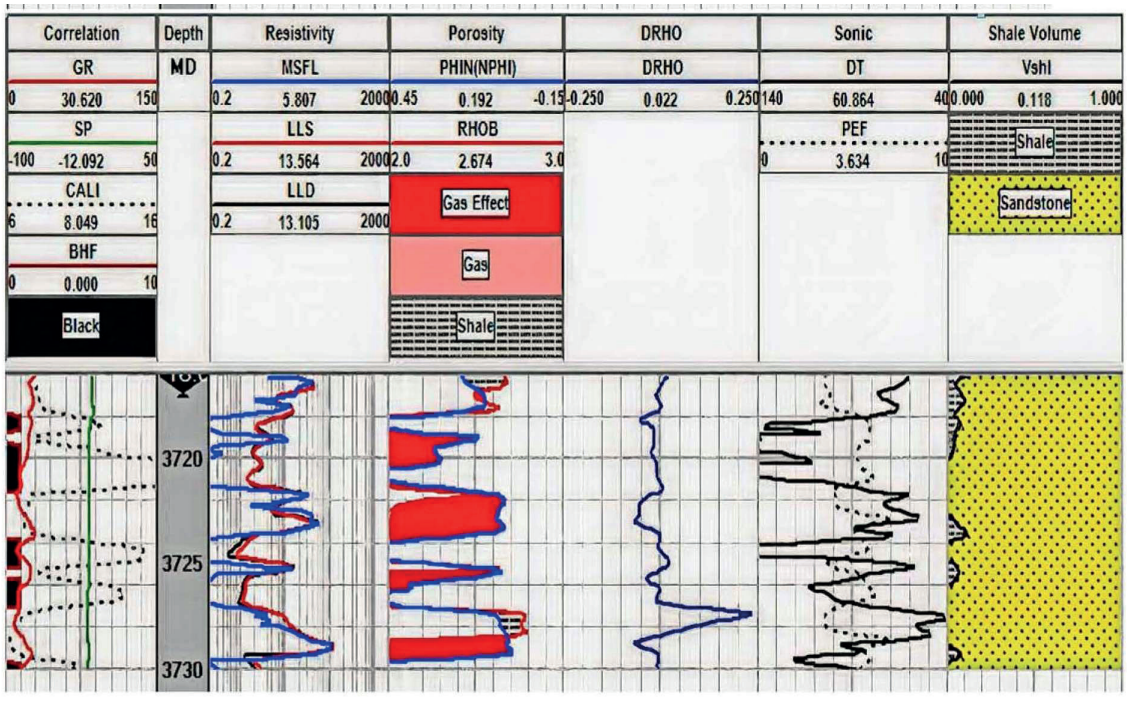

b

Fig. 2 - Reservoir of interest in zone-1 of the Meyal-8 well within the studied area, showing the appropriate reservoir interval zone.

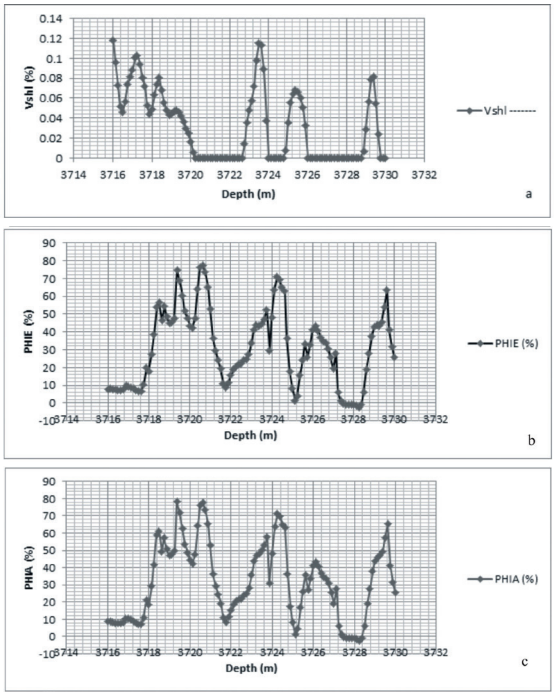

Fig. 3- V_{shl} (a), ϕ_e (b), and ϕ_a (c) of zone-1 of the Meyal-8 well.

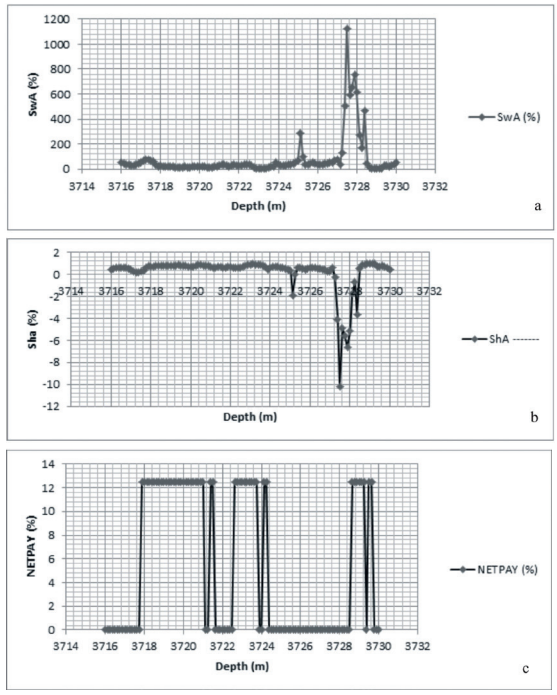

Fig. 4- Sw_A (a), Sh_A (b), and *NETPAY* (c) of zone-1 of the Meyal-08 well.

shale volume in zone-1 of the Meyal-10 well is 21.8% (y-axis) plotted against depth/m (x-axis) (Fig. 9a), ϕ_e is 14.68% (y-axis) plotted against depth/m (x-axis) (Fig. 9b), ϕ_a is 19.1% (y-axis) plotted against depth/m (x-axis) (Fig. 9c), Sw_A is 43% (y-axis) plotted against depth/m (x-axis) (Fig. 10a), and Sh_A is 57% (y-axis) plotted against depth/m (x-axis) (Fig. 10b). By applying three cut-offs, V_{shl}, ϕ_e, and *Sw*, the maximum net pay is 5% (y-axis) plotted against depth/m (x-axis) (Fig. 8; Fig. 10c).

4.2. Cross- plot

The utilisation of cross-plots is very promising for the analysis of several measurements obtained simultaneously from the exploration of geological wells. Cross-plots serve as graphical representations that facilitate the identification of intricate patterns and relationships within complex data sets (Garland *et al*., 2012). Schlumberger *et al.* (1934) pioneered the construction of cross-plots by plotting well log compositions against depth (Liu, 2017). This technique provides a visual means of investigating the interplay between different log parameters and their variations with depth. The importance of this approach is well-documented in the literature, with studies highlighting its relevance in deciphering subsurface lithology, fluid content, and structural attributes (Tavakoli, 2018). By offering a comprehensive visualisation of data, cross-plots enable geoscientists and researchers to extract valuable insights into the geological composition and behavior of subsurface formations. Therefore, a detailed exploration of the cross-plot methodology, supported by pertinent literature, is essential for harnessing its potential in enhancing the understanding of subsurface environments.

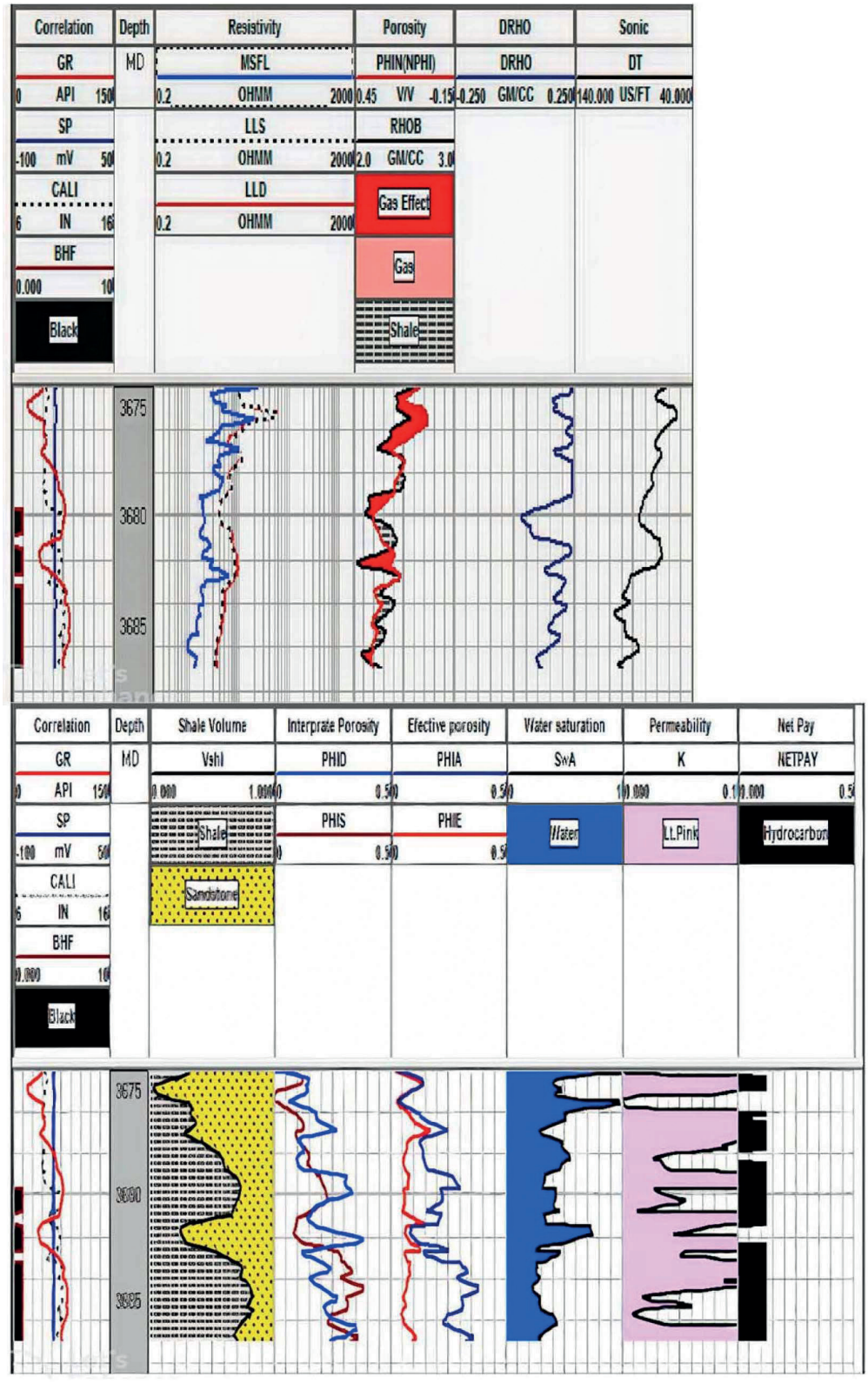

Fig. 5 - Reservoir of interest in zone-1 (red clays of the Chorgali Formation) of the Meyal-09 well.

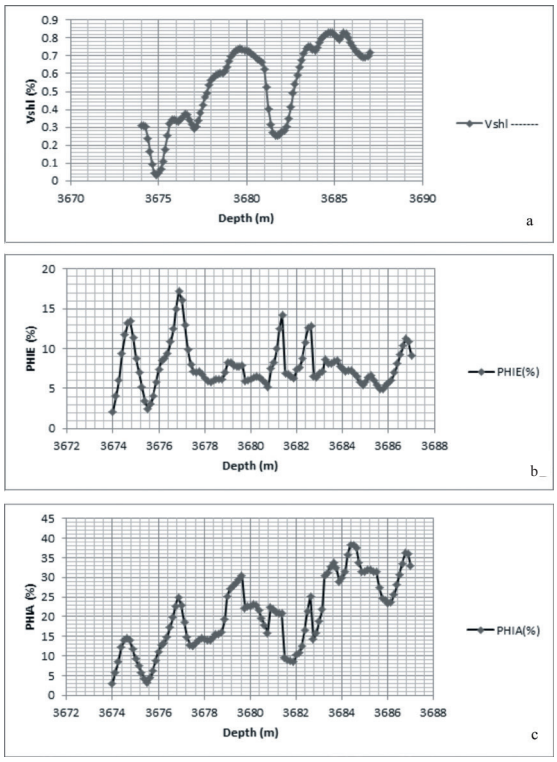

Fig. 6 - V_{shl} (a), ϕ_e (b), and ϕ_a (c) in zone-1 of the Meyal-09 well.

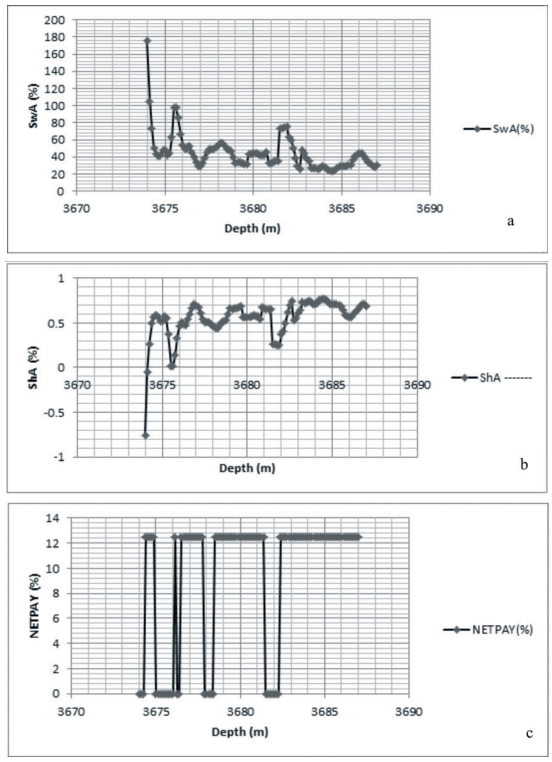

Fig. 7 - Sw_A (a), Sh_A (b), and *NETPAY* (c) in zone-1 of the Meyal-09 well.

4.2.1. Density and neutron-cross-plots

In lithology identification, density and neutron cross-plots have been used to evaluate the reservoir characteristics. ϕ_n and ρ_b are plotted against the x-axis and y-axis, respectively. In these wells, lithology and depth are plotted against each other on the basis of a cross-plot. The presence of calcite cement in sandstone can be slightly displaced towards the limestone line (Rider, 1996).

ρ_b and ϕ_n cross-plot of the Meyal-08 well**.** To understand the basic lithology of the Chorgali Formation, the ρ_b and ϕ_n cross-plot has been used. In Fig. 11a, limestone (LS), is demarked by the central green line, sandstone (SS) by the upper blue line, and dolomite (DM) by the lower red line.

ρ_b and ϕ_n cross-plot of the Meyal-09 well. To understand the basic lithology of the Chorgali Formation, the ρ_b and ϕ_n cross-plot has been used. In Fig. 11b, limestone (LS) is demarked by the central green line, sandstone (SS) by the upper blue line, and dolomite (DM) by the lower red line.

ρ_b and ϕ_n cross-plot of Meyal-10. To understand the basic composition of the Chorgali Formation, the ρ_b and ϕ_n cross-plot has been used. In Fig. 11c, limestone (LS) is demarked by the central green line, sandstone (SS) by the upper blue line, and dolomite (DM) by the lower red line.

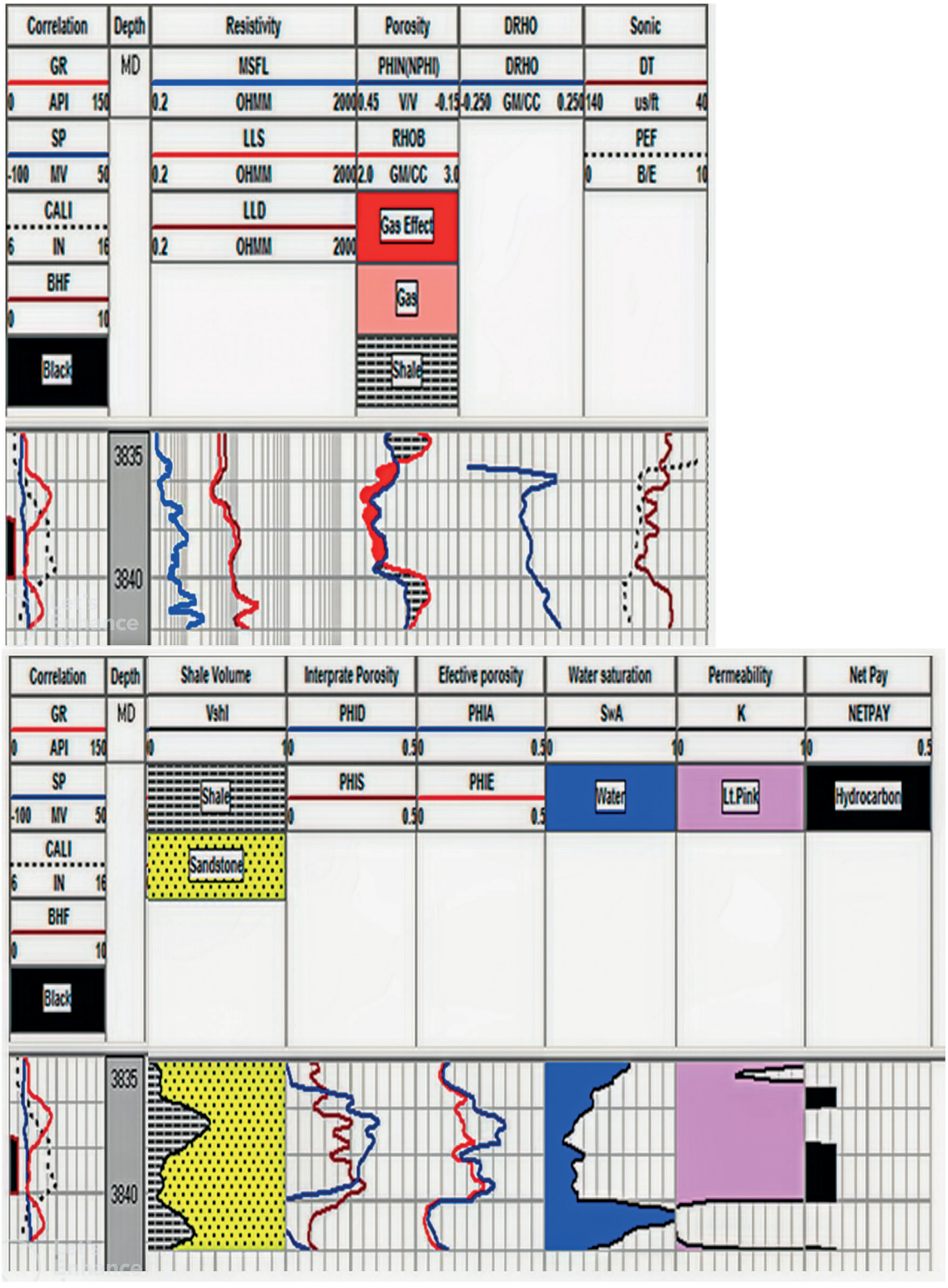

Fig. 8 - Reservoir of interest in zone-1 (the Chorgali Formation) of the Meyal-10 well.

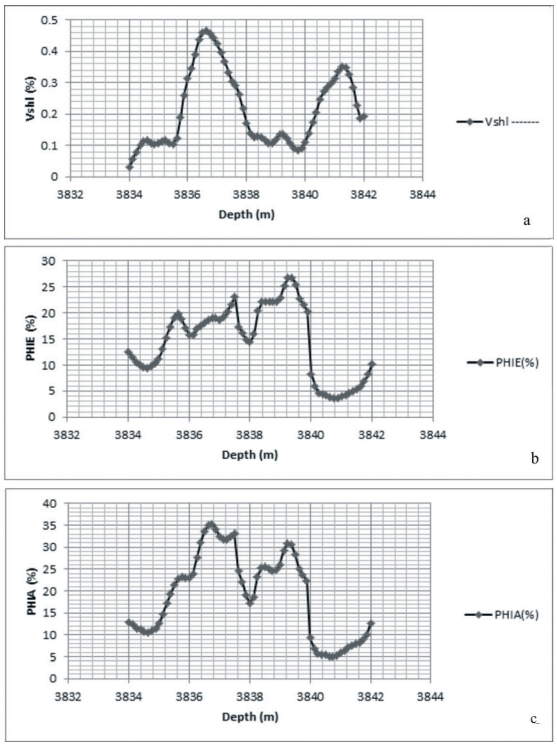

Fig. 9 - V_{shl} (a), ϕ_e (b), and ϕ_a (c) in zone-1 of the Meyal-10 well.

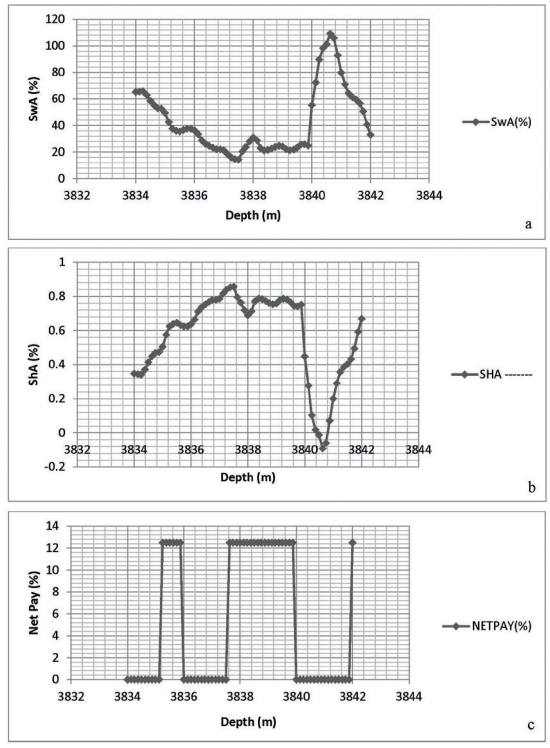

Fig. 10 - Sw_A (a), Sh_A (b), and *NETPAY* (c) in zone-1 of the Meyal-10 well.

4.3. Correlation

Correlation is a significant geological technique that provides evidence of the variations that have taken place at different stages of the Earth's history. It is the comparison between the rock units of similar ages in various areas. It also indicates the times at which such changes have occurred (Khan *et al.*, 2017). Structural and stratigraphic analysis has been used for subsurface investigation.

Stratigraphic correlation is used to compare geologic phenomena based on rock type. In such a correlation, the rock of one area is correlated with the rocks of another area. A relationship was established between all three wells, i.e. the Meyal-08, Meyal-09, and Meyal-10, so as to understand the stratigraphic record of the study area.

The datum line is taken from the top of the Sakesar Limestone of these three wells. The total depth of the Meyal-08 well is 3,810.30 m. The stratigraphy of the well ranges from Eocene (Sakesar Limestone, Chorgali Formation) to Pliocene (Nagri Formation), whereas the total depth of the Meyal-09 well is 4,123.10 m, and that of the Meyal-10 well is 4,303.90 m.

The Chorgali Formation, of Eocene age, is the producing reservoir in the Meyal-08 (14 m thick), Meyal-09 (13 m thick), and Meyal-10 (8 m thick) wells with good hydrocarbon potential (20.79%, 55.56%, and 57%, respectively). As the effective porosity in the Chorgali Formation can be enhanced by the impact of fracturing, these processes could increase oil production. The rock unit in Meyal-09 ranges from the Upper Rani Kot and Patala Formation, whereas in Meyal-10 the rock units range from the Datta Formation (Early Jurassic) to Nagri Formation (Pliocene). All three wells have been correlated based on lithological similarity (Fig. 12).

4.4. Discussion

The discussion section not only serves as a platform for presenting results but also provides a valuable opportunity for contextualising and comparing the findings. By juxtaposing the obtained results with those from similar studies in the region, as well as by drawing parallels with international literature, a deeper understanding of the implications and significance of the outcomes can be achieved. In the Meyal-08 well, for instance, the identified reservoir zone within

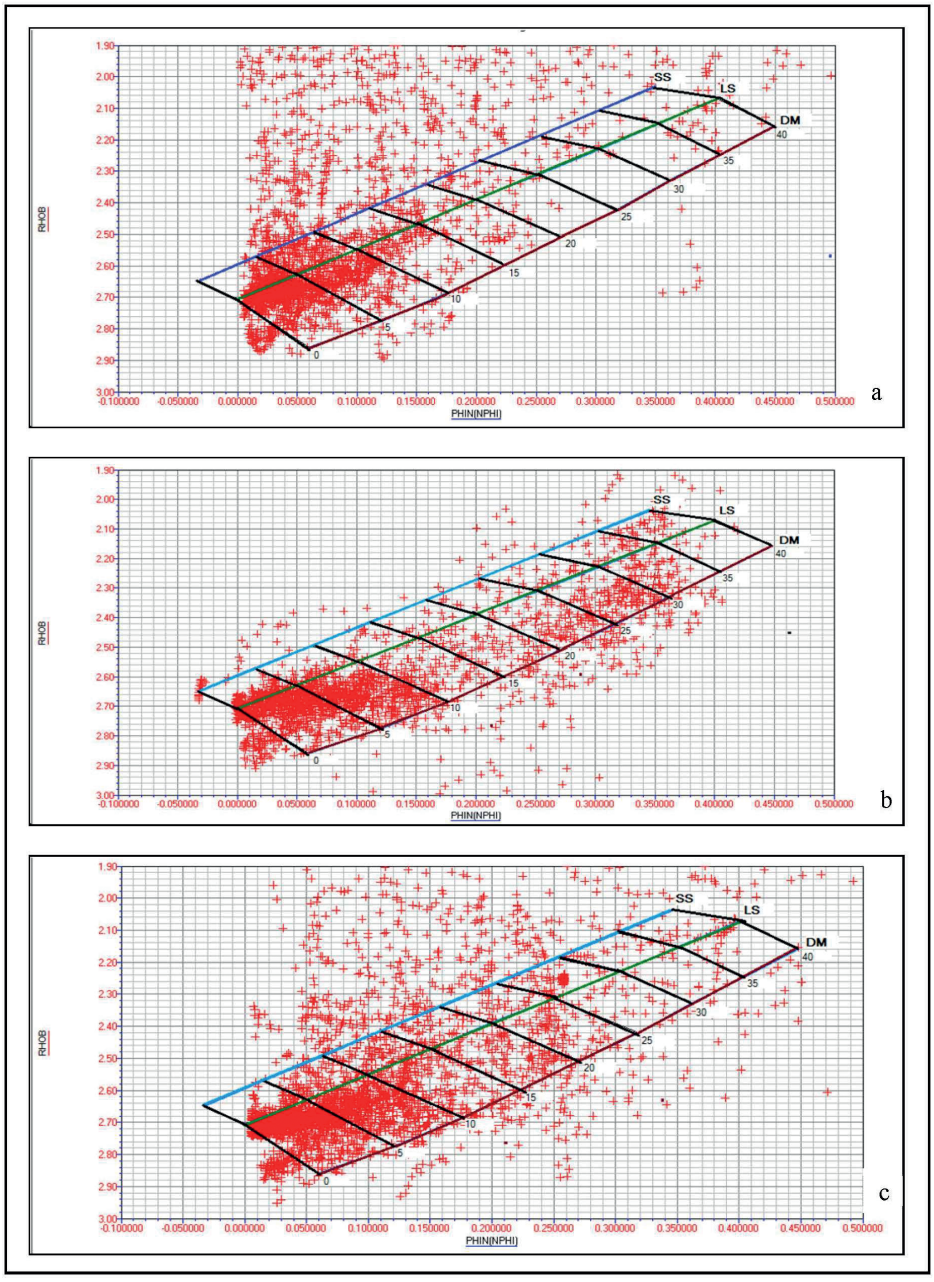

Fig. 11- Cross-plot of zone-1 of the: a) Meyal-08 well; b) Meyal-09 well; and c) Meyal-10 well. SS = sandstone; LS = limestone; DM = dolomite.

the Chorgali Formation demonstrates intriguing characteristics, such as an average V_{shl} of 3.1% and a porosity of 32.09%, which can be compared with analogous formations in neighbouring fields (Johnson and Brown, 2021; Pang *et al.*, 2021). This contextualisation provides insights into

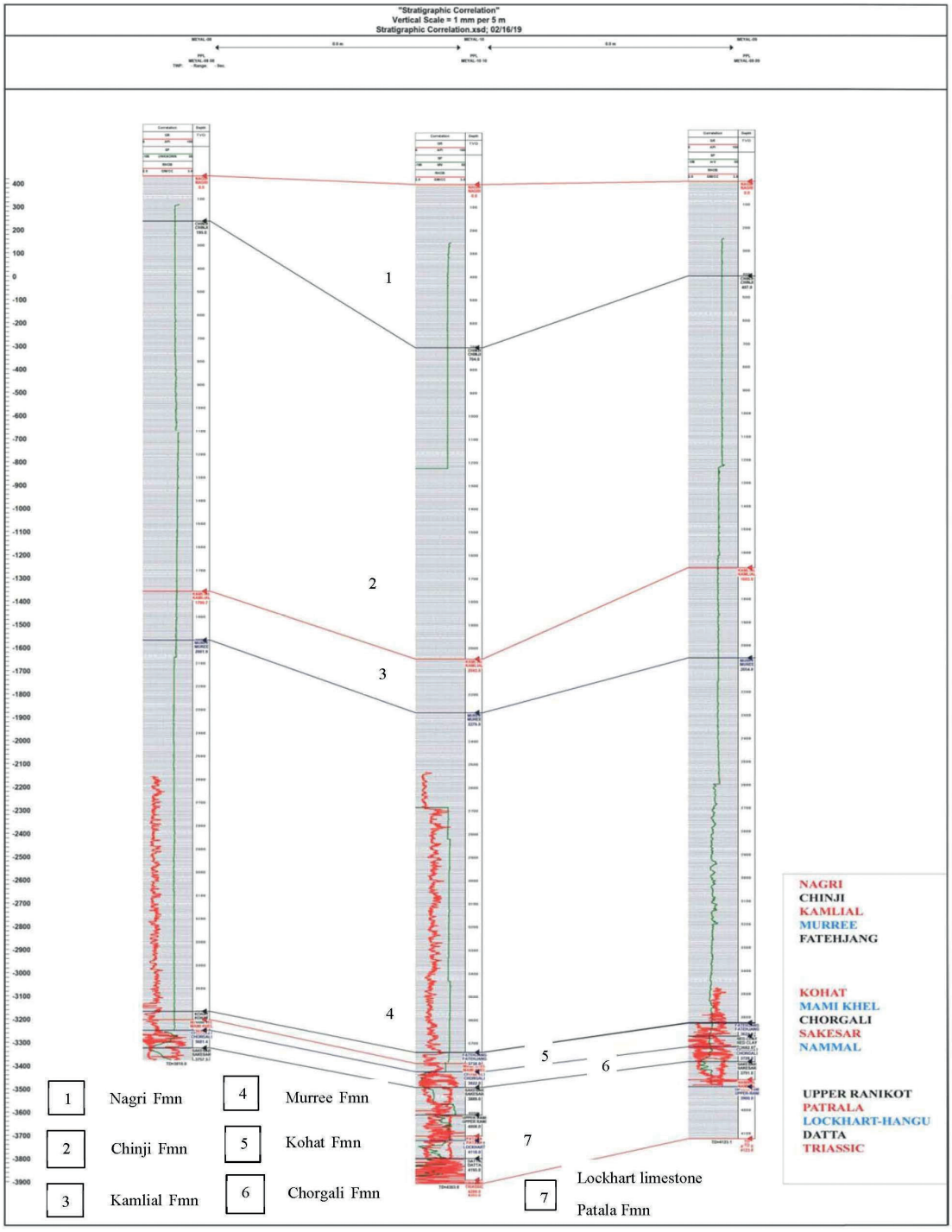

Fig. 12 - Log correlation between the Meyal-08, Meyal-09, and Meyal-10 wells.

the variability and uniqueness of the Meyal reservoir. Similarly, the considerable V_{shl} value of 53.79%, observed in the Meyal-09 zone of interest could be compared with V_{shl} values reported in formations with similar lithological compositions (Tavakoli, 2018).

Moreover, from a comparison of the hydrocarbon saturation values across the three wells, Meyal-10 stands out with an average saturation of 57%, potentially indicating distinct reservoir dynamics (Tolmachev *et al.*, 2020). It is noteworthy that the applied petrophysical parameters, such as porosity and water saturation, significantly influence the estimation of net pay, as evidenced by the variations observed in the Meyal-09 zone of interest. These inter-comparisons shed light on the reliability of the applied methodologies and their adaptability to specific geological settings.

By globally extending the comparison, the current blow-down stage of the Meyal field aligns with production trends observed in similar fields across the globe. The extraction of liquified petroleum gas and fuel, in addition to oil and gas, underscores the multifaceted nature of hydrocarbon recovery from reservoirs in similar stages (Patel and Gupta, 2017). Furthermore, the successful utilisation of horizontal drilling techniques in the Jurassic reservoir resonates with international practices in enhancing field productivity (Lei *et al.*, 2022). In essence, comparing the obtained results with local and international studies enriches the understanding of the unique characteristics and global relevance of the Meyal field reservoir dynamics.

5. Conclusions

The main hydrocarbon potential lies in the Chorgali Formation, which serves as the prime reservoir rock. Additionally, the Patala Shale and Chorgali formations play integral roles as source rocks. This intricate interplay between reservoir and source rocks reveals the multifaceted nature of hydrocarbon generation and accumulation within the Meyal oil field.

Almost 80% of hydrocarbon production has been produced from the Chorgali Formation and Sakessar Limestone (Eocene), while 20% of oil has been produced from the Ranikot Formation, Lockhart Limestone, and Datta Sandstone, having heterogeneous compositions (poor characteristics). Petrophysical analysis confirms that the Chorgali Formation acts as a reservoir with a 3% to 21% volume of shale.

The volumetric shale content, ranging from 3% to 21%, plays a pivotal role in influencing the overall characteristics and productivity of the reservoir. The average porosity and effective porosity of the Chorgali Formation vary from 19% to 32% and from 7% to 14%, respectively. Average water saturation varies from 43% to 79% (economically recovered from the reservoir). Conversely, the calculated net pay varies from 5% to 53%, denoting the thickness of the reservoir interval with economically viable hydrocarbon content, and the average hydrocarbon saturation varies from 20% to 57% in the wells studied. Evaluated results show that Meyal-08, Meyal-09, and Meyal-10 are oil-bearing wells.

The current study proves that the wells are capable of economically producing hydrocarbons. The capacity of the wells to yield hydrocarbons in an economically feasible manner is a testament to their potential as valuable assets within the Meyal oil field. This study empowers stakeholders with the insights needed to make informed decisions regarding extraction strategies, field management, and resource optimisation, ensuring the sustained productivity of the Meyal oil field for years to come.

Acknowledgments. The data used in the current study were provided through the courtesy of the Director General Petroleum Concession, and the Ministry of Petroleum Pakistan from Landmark Resources. The authors acknowledge the Department of Earth Sciences,University of Sargodha, Sargodha, Pakistan for providing the basic facilities as well as the Oil and Gas Development Company Limited (OGDCL), Islamabad, for providing technical expertise and software facilities. The present research work was funded by the authors.

REFERENCES

Aamir M. and Siddiqui M.M.; 2006: *Interpretation and visualization of thrust sheets in a triangle zone in eastern Potwar, Pakistan.* The Leading Edge, 25, 24-37, doi: 10.1190/1.2164749.

Abir I.A., Khan S.D., Ghulam A., Tariq S. and Shah M.T.; 2015: *Active tectonics of western Potwar Plateau - Salt Range, northern Pakistan from InSAR observations and seismic imaging.* Remote Sensing of Environment, 168, 265-275, doi: 10.1016/j.rse.2015.07.011.

Ahmed N., Kashif M., Dou B., Tariq M., Us M.S. and Ullah Z.; 2023: *Prediction of paleoclimate of Eocene salt, Kohat Basin, Khyber Pakhtunkhwa, Pakistan*. Episodes, 46, doi: 10.18814/epiiugs/2022/022017.

Akhter G., Khan Y., Bangash A.A., Shahzad F. and Hussain Y.; 2018: *Petrophysical relationship for density prediction using Vp & Vs in Meyal oilfield, Potwar sub-basin, Pakistan.* Geodesy and Geodynamics, 9, doi: 10.1016/j.geog.2017.07.008.

Ali J., Ashraf U., Anees A., Peng S., Umar M.U., Vo Thanh H., Khan U., Abioui M., Mangi H.N., Ali M. and Ullah J.; 2022: *Hydrocarbon potential assessment of carbonate-bearing sediments in a Meyal Oil Field, Pakistan: insights from logging data using machine learning and Quanti Elan modeling.* ACS Omega, *7*, 39375-39395, doi: 10.1021/acsomega.2c05759.

Amjad M.R., Ehsan M., Hussain M., Al-Ansari N., Rehman A., Naseer Z., Ejaz M.N., Baouche R. and Elbeltagi A.; 2023: *Carbonate reservoir quality variations in basins with a variable sediment influx: a case study from the Balkassar Oil Field, Potwar, Pakistan.* ACS Omega, 8, 4127-4145, doi: 10.1021/acsomega.2c06773.

Asquith G., Krygowski D., Henderson S. and Hurley N.; 2004: *Basic well log analysis*. American Association of Petroleum Geologists, Tulsa, OK, USA, 244 pp., doi: 10.1306/Mth16823.

Awais M.; 2015: *Reservoir evaluation of the Eocene Chorgali Formation using Outcrop data and Geophysical logs of Meyal Oil Field, Potwar Plateau, Pakistan.* Unpublished MS Thesis in Geological Sciences, National Centre of Excellence in Geology, University of Peshawar, Pakistan.

Awais M., Hanif M., Khan M.Y., Jan I.U. and Ishaq M.; 2019: *Relating petrophysical parameters to petrographic interpretations in carbonates of the Chorgali Formation, Potwar Plateau, Pakistan.* Carbonates Evaporites, 34, 581–595, doi: 10.1007/s13146-017-0414-x.

Awais M., Hanif M., Jan I.U., Ishaq M. and Khan M.Y.; 2020: *Eocene carbonate microfacies distribution of the Chorgali Formation, Gali Jagir, Khair-e-Murat Range, Potwar Plateau, Pakistan: approach of reservoir potential using outcrop analogue.* Arabian Journal of Geosciences, 13, 18 pp., doi: 10.1007/s12517-020-05377-9.

Bagheri M. and Rezaei H.; 2019: *Reservoir rock permeability prediction using SVR based on radial basis function kernel.* Carbonates and Evaporites, 34, doi: 10.1007/s13146-019-00493-4.

Bahar A. and Kelkar M.; 2000: *Journey from well logs/cores to integrated geological and petrophysical properties simulation: a methodology and application.* SPE Res Eval & Eng, 3, doi: 10.2118/66284-PA.

Cheng H., Wei J. and Cheng Z.; 2022: *Study on sedimentary facies and reservoir characteristics of Paleogene sandstone in Yingmaili block, Tarim basin.* Geofluids, 3, 14 pp., doi: 10.1155/2022/1445395.

Chongwain G.M., Osinowo O.O., Ntamak-Nida M.J. and Nkoa P.E.N.; 2018: *Seismic attribute analysis for reservoir description and characterization of M-Field, Douala sub-basin, Cameroon.* Advances In Petroleum Exploration and Development, 15, doi: 10.3968/10220.

Dolson J.; 2016: *Basic log analysis, quick-look techniques, pitfalls and volumetrics.* In: Dolson J. (ed), Understanding oil and gas shows and seals in the search for hydrocarbons, Springer International Publishing, Cham, Switzerland, pp. 315-347, doi: 10.1007/978-3-319-29710-1_6.

Duroy Y., Farah A. and Lillie R.J.; 1989: Subs*urface densities and lithospheric flexure of the Himalayan foreland in Pakistan.* In: Malinconico L.L. Jr. and Lillie R.J. (eds), Tectonics of the western Himalayas, GSA, Special Paper no. 232, pp. 217-236, doi: 10.1130/SPE232-p217.

Durrani M.Z.A., Rahman S.A., Talib M., Subhani G. and Sarosh B.; 2022: *Characterization of seismic anisotropy using azimuthal AVO analysis (AVAz) - An application case study in the deep and tight carbonate reservoirs from Potwar Basin onshore Pakistan.* Journal of Applied Geophysics, 205, doi: 10.1016/j.jappgeo.2022.104767.

Faisal M., Rehman F., Rehman S. and Ahsan N.; 2013: *Better perceptive and enhanced visualization of seismic profiles for the exploration of hydrocarbon using a seismic and synthetic seismogram modeling of Khipro block, southern Indus basin, Sindh province, Pakistan*. Energy Sources, Part A, 35, 2101-2112, doi: 10.1080/15567036.2010.531511.

Garland J., Neilson J., Laubach S.E. and Whidden K.J.; 2012: *Advances in carbonate exploration and reservoir analysis.* Special Publications, Geological Society, London, 370, 15 pp., doi: 10.1144/SP370.15.

Hasany S.T. and Saleem U.; 2012: *An integrated subsurface geological and engineering study of Meyal Field, Potwar Plateau, Pakistan.* Search and Discovery Article, article no. 20151, 41 pp.

Hill D.G.; 2017: *Formation evaluation*. In: Hsu C.S. and Robinson P.R. (eds), Springer Handbook of Petroleum Technology, Springer International Publishing, Cham, Switzerland, pp. 433-500, doi: 10.1007/978-3-319-49347-3.

Iqbal S., Akhter G. and Bibi S.; 2015: *Structural model of the Balkassar area, Potwar Plateau, Pakistan.* International Journal of Earth Sciences, 104, 2253-2272, doi: 10.1007/s00531-015-1180-4.

Johnson R.K. and Brown S.M.; 2021: *Lithological variability and petrophysical parameters in nearby fields*. Geoscience Quarterly, 48, 67-82.

Kadkhodaie-Ilkhchi A. and Kadkhodaie-Ilkhchi R.; 2018: *A review of reservoir rock typing methods in carbonate reservoirs: relation between geological, seismic, and reservoir rock types.* Iranian Journal of Oil and Gas Science and Technology, 7, 13-35.

Khan M.A., Ahmed R., Raza H.A. and Kemal A.; 1986: *Geology of petroleum in Kohat-Potwar depression, Pakistan.* AAPG Bull., 70, 396-414, doi: 10.1306/9488571E-1704-11D7-8645000102C1865D.

Khan M.Z., Rahman Z.U., Khattak Z. and Ishfaque M.; 2017: *Microfacies and diagenetic analysis of Chorgali carbonates, Chorgali Pass, Khair-e-Murat Range: implications for hydrocarbon reservoir characterization.* Pakistan Journal of Geology, 1, 18-23.

Lei Q., Xu Y., Cai B., Guan B., Wang X., Bi G., Li H., Li S., Ding B., Fu H., Tong Z., Li T. and Zhang H.; 2022: *Progress and prospects of horizontal well fracturing technology for shale oil and gas reservoirs.* Petroleum Exploration and Development, 49, 191-199, doi: 10.1016/S1876-3804(22)60015-6.

Liu H.; 2017: *Principles and applications of well logging.* Springer, Berlin Heidelberg, Germany, 356 pp., doi: 10.1007/978-3-662-54977-3.

Mehmood M., Yaseen M., Din I.U., Khan M.J., Ullah T. and Anwar-ul-Haq; 2018: *Petrophysical parameters estimation and reservoir characterisation based on well log data in the Joya Mair Oil Field, Minwal X-01 Well, Potwar Sub-Basin and Upper Indus Basin of Pakistan.* Global Journal of Earth Environmental Science, 3, 44-55, doi: 10.31248/GJEES2018.023.

Mokheimer E.M., Hamdy M., Abubakar Z., Shakeel M.R., Habib M.A. and Mahmoud M.; 2019: *A comprehensive review of thermal enhanced oil recovery: techniques evaluation.* Journal of Energy Resources Technology, 141, doi: 10.1115/1.4041096.

Moosavi N., Bagheri M., Nabi-Bidhendi M. and Heidari R.; 2022: *Fuzzy support vector regression for permeability estimation of petroleum reservoir using well logs*. Acta Geophysica, 70, 161-172, doi: 10.1007/s11600-021-00700-8.

Moosavi N., Bagheri M., Nabi-Bidhendi M. and Heidari R.; 2023: *Porosity prediction using fuzzy SVR and FCM SVR from well logs of an oil field in south of Iran*. Acta Geophysica, 71, 769-782, doi: 10.1007/s11600-022-00944-y.

Pang X., Shao X., Li M., Hu T., Chen Z., Zhang K., Jiang F., Chen J., Chen D., Peng J., Pang B. and Wang W.; 2021: *Correlation and difference between conventional and unconventional reservoirs and their unified genetic classification.* Gondwana Research, 97, 73-100.

Rehman F., Rehman S., Ullah M.F., Kashif M., Ahsan N. and Abbas M.; 2014: *Conjecturing gross lithologici information using elastic moduli obsessed by rock physics as tool. A case study for Khewra sandstone, Fortabbas area, Pakistan.* Energy Sources, Part A, 36, 1786-1792, doi: 10.1080/15567036.2011.559527.

Rider M.; 1996: *The geological interpretation of well logs, 2nd edit*. Whittles Publ., Dunbeath, Caithness, Scotland, UK, 280 pp.

Sajid M., Kashif M., Zahid M.A., Javed A. and Shaikh A.; 2021: *Petrophysical evaluation of reservoir rocks of Rajian-01, Daiwal-01, and Kal-01 by well log data, Potwar Plateau, upper Indus basin, Pakistan*. Boll. Geof. Teor. Appl., 62, 135-158, doi: 10.4430/bgta0340.

Sameeni S.J., Ahmad A., Ahmad N. and Ahsan N.; 2013: *Biostratigraphy of Chorgali Formation, Jhalar area, Kala Chitta range, northern Pakistan.* Sci. Int., 25, 567-577.

Schlumberger C., Schlumberger M. and Leonardon E.G.; 1934: *A new contribution to subsurface studies by means of electrical measurements in drill holes.* Transactions of the AIME, 110, 273-289, doi: 10.2118/934273-G.

Shah S.B.A. and Abdullah W.H.; 2016: *Petrophysical properties and hydrocarbon potentiality of Balkassar well 7 in Balkassar oilfield, Potwar Plateau, Pakistan*. Bull. Geol. Soc. Malaysia., 62, 73–77.

Shi K., Pang X., Chen J., Hui S., Yuan W., Chen J., Hu T., Li M., Zhang K., Liu Y., Zhang S. and You T.; 2023: *Pore structure characteristics and evaluation of carbonate reservoir: a case study of the Lower Carboniferous in the Marsel exploration area, Chu-Sarysu Basin.* Natural Resources Research, 32, 771-793, doi: 10.1007/s11053-023-10166-8.

Singh N.P.; 2019: *Permeability prediction from wireline logging and core data: a case study from Assam - Arakan basin.* J. Petrol Explor Prod Technol, 9, 297-305, doi: 10.1007/s13202-018-0459-y.

Tavakoli V.; 2018: *Geological core analysis: application to reservoir characterization.* Springer, Cham, Switzerland, 99 pp., doi: 10.1007/978-3-319-78027-6.

Tolmachev O., Urunov A., Muminova S., Dvoichenkova G. and Davydov I.; 2020: *Review of unconventional hydrocarbon resources: production technologies and opportunities for development.* Mining of mineral deposits, 14, 113-121.

Ullah H., Jianhua Z., Kashif M., Room S.A.E., Zafar Z. and Rehman S.U.; 2023: *Characteristics and prediction of paleo-environment of Eocene Jatta Gypsum, Kohat Basin, Pakistan.* Arabian Journal of Geosciences, 16, 19 pp., doi: 10.1007/s12517-023-11415-z.

Wolf D., Bernor R.L. and Hussain T.; 2013: *A systematic, biostratigraphic and paleobiogeographic reevaluation of the Siwalik hipparionine horse assemblage from the Potwar Plateau, northern Pakistan.* Paleontographica, 300, 1-115, doi: 10.1127/pala/300/2013/1.

Yasin Q., Baklouti S., Khalid P., Ali S.H., Boateng C.D. and Du Q.; 2021: *Evaluation of shale gas reservoirs in complex structural enclosures: a case study from Patala Formation in the Kohat-Potwar Plateau, Pakistan.* Journal of Petroleum Science and Engineering, 198, 21 pp., doi: 10.1016/j.petrol.2020.108225.

Zhao Q., Li X. S, Chen Z.Y., Xia Z.M. and Xiao, C.W.; 2024: *Numerical investigation of production characteristics and interlayer interference during co-production of natural gas hydrate and shallow gas reservoir*. Applied Energy, 354, doi: 10.1016/j.apenergy.2023.122219.

Zhu N., Yao S., Zhang Y., Ning S., Jia B., Zhou Y. and Zhang W.; 2024: *Influence of coupled dissolution-precipitation processes on the pore structure, characteristics, and evolution of tight sandstone: a case study in the upper Paleozoic reservoir of Bohai Bay Basin, eastern China.* Journal of Asian Earth Sciences, 262, 16 pp., doi: 10.1016/j.jseaes.2023.105998.

Corresponding author: Muhammad Kashif
Department of Earth Sciences, University of Sargodha
University road, Sargodha 40100, Pakistan
Phone: +92 334 6893113, e-mail: kashifyaqub@yahoo.com